Nature of prominences and their role in Space Weather
Proceedings IAU Symposium No. 300, 2013
B. Schmieder, J.-M. Malherbe & S. T. Wu, eds.

doi:10.1017/S1743921313010703

Prominence Seismology

J. L. Ballester

Departament de Física, Universitat de les Illes Balears,
E - 07122, Palma de Mallorca, Spain
email: joseluis.ballester@uib.es

Abstract. Quiescent solar prominences are cool and dense plasma clouds located inside the hot and less dense solar corona. They are highly dynamic structures displaying flows, instabilities, oscillatory motions, etc. The oscillations have been mostly interpreted in terms of magnetohydrodynamic (MHD) waves, which has allowed to perform prominence seismology as a tool to determine prominence physical parameters difficult to measure. Here, several prominence seismology applications to large and small amplitude oscillations are reviewed.

Keywords. Prominence Oscillations, MHD Waves

1. Introduction

Seismology refers to the process of deriving the physical conditions of a medium by analysing properties of the oscillations or the waves travelling through the medium. Helioseismology was invented almost 50 years ago, and became an efficient tool to probe the internal structure of the Sun, while thanks to space-based high-resolution observations, which provided with strong evidence about the presence of oscillations and waves in coronal magnetic structures, Solar Atmospheric Seismology, proposed by Rosenberg (1970), Uchida (1970) and Roberts *et al.* (1984), became a reality about 15 years ago.

MHD waves and oscillations provide with an indirect path to determine physical parameters [coronal magnetic field, transport coefficients (viscosity, resistivity, thermal conductivity, etc.), heating function, filling factors, inhomogeneity scale] of the solar corona. Therefore, MHD seismology is a method of remote diagnostics of plasma structures combining observations of oscillatory motions with an interpretation in terms of MHD waves.

MHD seismology involves the solution of the forward and inverse problems. In the forward problem, a theoretical model is built and used to predict the oscillations of many different modes. If the predictions do not agree with observations, then, we modify the model somehow and start again the comparison. On the contrary, in the inverse problem, instead of computing frequencies from a theoretical model, we construct the model from the observed frequencies. MHD seismology is similar to helioseismology, but with a few differences:

(*a*) Only a local diagnostics of the oscillating structures and their nearest vicinity (local seismology) is obtained

(*b*) Three wave modes are available: fast, slow magnetoacoustic and Alfvén

Prominence seismology was initially suggested by Roberts & Joarder (1994):"*...the possibility of using data on the modes of oscillation of a prominence to derive seismic information about the structure of the prominence...*" and by Vial (1998):"*...we may well be en route towards prominence seismology*", and its main aim is to determine physical parameters difficult to measure by other methods. The observational tools available for prominence seismology are:

(*a*) Large amplitude oscillations, with velocity amplitudes greater than 20 km/s. [Tripathi *et al.* (2009)]

(*b*) Small amplitude oscillations, whose velocity amplitudes range from the noise level up to a few km/s. [Arregui *et al.* (2012)]

2. Prominence seismology using large amplitude oscillations

The first seismological study was made by Hyder (1966) using observational data about large amplitude oscillations of 11 filaments reported by Ramsey & Smith (1966). Assuming that the filaments are located in a depressed magnetic field, these observations were interpreted in terms of vertical oscillations damped by the viscosity of the surrounding coronal plasma, and estimates of the radial magnetic field in the range $2-30$ G were obtained. Furthermore, the coronal coefficient of viscosity was also determined. Kleczek & Kuperus (1969) re-interpreted the above mentioned observations in terms of horizontal (transverse) oscillations of filaments. They assumed that a line-tied magnetic field was directed along the filament, that the restoring force was provided by magnetic tension and that the oscillations were damped by the emission of acoustic waves. Then, from the equation of motion of a damped harmonic oscillator, the period is given by

$$P = 4\pi L B^{-1}\sqrt{\pi\rho_p}$$

Knowing the period of oscillation (P), measuring the length of the filament (L) and assuming a typical density (ρ_p), the strength of the magnetic field (B) can be determined. Nowadays, this model is still being used to explain prominence oscillations and to perform prominence seismology.

Transverse oscillations have been also observed in a pre-erupting filament (Isobe & Tripathi (2006)). These oscillations were present along one foot of a polar crown filament, prior to the eruption of the full structure. The oscillating part of the filament moved like a rigid body with a line-of-sight velocity amplitude > 20 km/s, a displacement amplitude ~ 20 - 30 arcsec, and a period ~ 2 hr. Following the theoretical model by Kleczek & Kuperus (1969), the magnetic field strength (9.8 G) and the Alfvén speed (87 km/s) were determined.

Longitudinal oscillations consist of periodic motions along the axis of a filament. Jing *et al.* (2003) and Jing *et al.* (2006) analysed several events reporting periods of 80, 160, 150, 100 min.; damping times of 210, 600, 450 min., maximum velocity amplitudes of 80, 50, 30, 100 km/s and maximum displacement amplitudes of 140, 160, 100, 80 Mm. These oscillations seem to be triggered by subflares, flares, filament eruption and reconnection events which happen close to the filaments. Vršnak *et al.* (2007) reported Hα observations of longitudinal oscillations in a filament with an initial displacement of 24 Mm, an initial velocity amplitude of 51 km/s, a period of 51 min. and a damping time of 115 min. Assuming that the filament was embedded in a flux rope, Vršnak *et al.* (2007) suggested that the oscillations were triggered by additional poloidal flux injected at one of its legs creating a magnetic pressure gradient along the filament, which is the restoring force. After linearising the equation of motion, the expression for the longitudinal displacement (X), in dimensionless form, is:

$$\ddot{X} = -\frac{2v_{A\varphi}^2}{L^2}X$$

which provides with an expression for the period, $P \approx 4.4L/v_{A\varphi}$, as a function of the poloidal Alfvén speed ($v_{A\varphi}$) and the length of the filament (L). Then, knowing the period and the length of the filament, the poloidal Alfvén speed can be determined ($v_{A\varphi} = 100$ km/s). Furthermore, assuming a set of prominence densities, the poloidal magnetic field strengh is in the range 5-15 G, and measuring the pitch angle, the longitudinal magnetic field strength can be also obtained (10 - 30 G).

Recently, a theoretical model for large amplitude longitudinal oscillations in filaments has been proposed [Luna & Karpen (2012), Luna *et al.* (2012), Zhang *et al.* (2013)]. The scenario is the following: When an energetic event (a subflare, for instance) happens close to a filament, the injected energy evaporates plasma at the fluxtube footpoint closest to the energetic event. Then, the flow of hot plasma pushes the cold plasma condensations (threads) located at the dips of a sheared double arcade, and the longitudinal oscillations start. After some time, they lose coherence due to period differences. The restoring force is the projected solar gravity directed towards the bottom of the dip and since the magnetic tension in the dip must be larger than the weight of the threads, we have,

$$\frac{B^2}{R} - mng_0 \geqslant 0$$

where R is the radius of curvature, m the particle mass, n the particle density, and g_0 the gravity. On the other hand, since the oscillation is gravity driven:

$$\omega = \sqrt{\frac{g_0}{R}}$$

and combining the above two expressions, we obtain,

$$B \geqslant \sqrt{\frac{g_0^2 mn}{4\pi^2}} P$$

Then, again, knowing the period (P) and assuming a typical density (n), the strength of the magnetic field (B) can be determined (31 - 75 G for the threads considered). In this case, the damping of the oscillations has been attributed to thermal and mass accretion effects.

On the other hand, this model points out that if longitudinal oscillations are gravity driven, the seismological determination of the magnetic field would not be influenced by the radius of curvature of the magnetic field dips.

3. Prominence seismology using small amplitude oscillations

3.1. *Seismology of prominence slabs*

Seismology of prominence slabs was performed in order to infer prominence physical properties and the methodology was based on the identification of observed oscillations with theoretical eigenmodes. Régnier *et al.* (2001) observed an active region filament with SUMER/SoHO detecting oscillations covering different ranges of periods: < 5 min.; $6 - 20$ min.; > 40 min. and considered the possible theoretical modes that could explain their observations. The slab model with a uniform and inclined magnetic field by Joarder & Roberts (1993) was chosen. The dispersion relations for Alfvén modes and magnetoacoustic modes were considered, providing the frequency of six fundamental modes: the symmetric Alfvén, slow and fast kink modes and the antisymmetric Alfvén, slow and fast sausage modes, as a function of the prominence parameters. Observations provided with estimates for the width (8000 km) and length (63,000 km) of the filament, and assumptions on other parameters, such as the temperature of the filament (8000 K) and of its environment (10^6 K), the density of the slab (10^{12} cm^{-3}), the magnetic field strength (20 G) and for the angle between the magnetic field and the long axis of the slab (25°), were made. The dispersion relations were then solved by using these parameters and the corresponding periods were obtained and classified.

From the comparison between the observed and calculated frequencies, an identification method of the oscillation modes in the observed filament was presented. The method makes use of the fact that the frequency ratio of the fundamental even Alfvén mode to the fundamental odd Alfvén mode only depends on the ratio of the half-with of the slab to the half-length of the filament, which is a measurable quantity. The same applies to the frequency ratios involving the slow kink/sausage and fast kink/sausage modes. Parametric calculations for the frequencies as a function of the magnetic field strength and the inclination angle, while keeping the slab density constant, were next performed. A diagnostic of the observed filament is obtained by looking for the parameters values that enable the matching of theoretical and observed frequencies. By following this method, the angle between the magnetic field and the long axis of the slab is estimated to be 18°. Using this value, an algebraic relation for the magnetic field strength as a function of the slab density is derived.

A more involved and ambitious diagnostic, using the slab model, was performed by Pouget *et al.* (2006). The long duration and high temporal resolution observations with CDS/SoHO enabled these authors to detect and measure the entire range of periodicities theoretically expected in a filament. In particular both the short (less that 10 min) and the long ones (more than 40 min) are detected.

The detailed analysis of three filaments is presented. The seismic inversion technique closely follows that of Régnier *et al.* (2001), in the sense that the first step towards the diagnostic is the use of frequency ratios between fundamental even/odd (kink/sausage) modes. These ratios only depend on the ratio of the filament half-width to its half-length. Once this ratio is measured, with a given uncertainty, Pouget *et al.* (2006) assume that their 16 hours long observation had allowed them to observe the six modes of interest, since the slowest mode is expected at a period of 5 hours, for standard prominence parameters.

The inversion method first assigns a possible triplet of measured frequencies to the 3 odd fundamental frequencies (odd Alfvén, slow sausage, and fast sausage modes). The coherence of each choice is examined against two tests. The first requires to find three corresponding even frequencies, with the condition that the even/odd frequency ratios are consistent with the measured half-width to half-length ratio. The second involves the inferred values for the density, temperature, magnetic field inclination angle, and magnetic field strength to be consistent with typical values reported in the literature. For each test, if the test was negative, the full triplet was changed and the series started again. On the contrary, if the tests succeeded, they considered that the six fundamental modes were identified.

The three filament observations led to coherent diagnostics and a single possible set of frequencies was found for each observation. The importance of this study is its ability to simultaneously determine the values of the inclination angle, temperature, and Alfvén speed for the same prominence. The drawback is that the modeling does not permit to capture the highly inhomogeneous nature of prominences.

Gravity is not considered in the above theoretical model, however, its inclusion produces a negligible effect on the prominence slab oscillations and seismological determinations.

3.2. *Seismology of filament threads*

Although quiescent prominences observed at the limb seem to be made of vertical threads (See Gunar's review in this volume), when observed on the disk as filaments they seem to be made by a myriad of fine structures which seem to be field aligned, outlining magnetic flux tubes [Engvold, (1998), Lin (2004), Lin *et al.* (2005), Lin *et al.* (2007),

https://doi.org/10.1017/S1743921313010703 Published online by Cambridge University Press

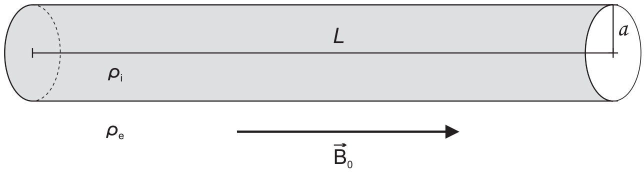

Figure 1. Sketch of an infinitely long thread immersed in the solar corona [Lin *et al.* (2009)].

Engvold (2008), Lin *et al.* (2008)]. These magnetic flux tubes are fully or partially filled with cold plasma condensations called threads [Lin (2004), Okamoto *et al.* (2007)], and the detected transverse thread oscillations, interpreted in terms of kink MHD waves, are used to perform thread seismology.

3.2.1. *Seismology using the period of filament thread oscillations*

Transverse thread oscillations observed by Lin *et al.* (2009) show evidence of waves propagating along individual threads. Ten of the swaying threads were chosen by Lin *et al.* (2009) for further investigation, and for each selected thread two or three perpendicular cuts were made in order to measure the properties of the propagating waves. Periods and amplitudes of the waves, as well as their phase velocity, were derived for each thread. Lin *et al.* (2009) interpreted the observed events as propagating MHD kink waves supported by the thread body. This mode is the only one producing a significant transverse displacement of the cylinder axis. In addition, it also produces short-period oscillations of the order of minutes, compatible with the observed periods. This interpretation also implies that the measured phase velocity is equal to the kink speed.

If an infinitely long, straight, cylindrical thread model, with the tube fully filled with cool and dense material, is assumed (Figure 1), a comparison between the observed wave properties and the theoretical prediction can be made. This enabled Lin *et al.* (2009) to obtain estimates for some physical parameters of interest, namely the Alfvén speed and the magnetic field strength in the studied threads. Assuming the thin tube approximation, length of the magnetic flux tube, L, much greater than the radius, a, and that inside and outside the magnetic flux tube the density is given by,

$$\rho_0(r) = \begin{cases} \rho_f, & r \leqslant a \\ \rho_c, & r > a \end{cases}$$

the kink speed, c_k, is,

$$c_k = \sqrt{\frac{2B_0^2}{\mu(\rho_f + \rho_c)}}$$

where μ is the magnetic permittivity, and the above expression can be written as,

$$c_k = v_{Af}\sqrt{\frac{2c}{c+1}}$$

with

$$\xi = \frac{\rho_f}{\rho_c}$$

and when this ratio becomes very large, then

$$c_k \sim \sqrt{2}v_{Af}$$

where v_{Af} is the thread Alfvén speed. The results for the internal Alfvén speed show a strong dispersion, suggesting that the physical conditions in different threads were very different in spite of belonging to the same filament. This result clearly reflects the highly inhomogeneous nature of solar prominences. Once the Alfvén speed in each thread was determined, the magnetic field strength could be computed after a value for the thread density was assumed.

3.2.2. *Seismology using the period and damping time of filament thread oscillations*

A feature clearly observed by Lin *et al.* (2009) is that the amplitudes of the waves passing through two different cuts along a thread are notably different. Apparent changes can be due to damping of the waves in addition to noise in the data. The damping of prominence oscillations is a common feature in many observed events and damping time-scales provide with an additional source of information that can be used when performing parameter inference using seismology inversion techniques. Among the different damping mechanisms which can be considered, resonant absorption in the Alfvén continuum seems a very plausible one and has been used to perform prominence thread seismology, using the damping as an additional source of information.

The model considered here is a one-dimensional infinitely long thread of mean radius a surrounded by a thin transition sheath of thickness l in which a smooth transition from the thread to the coronal density takes place. The thread is located inside a flux tube, in static equilibrium, gravity is neglected, the magnetic field is uniform inside and outside and the low-β approximation is considered. The thread plasma density is ρ_f, the coronal plasma density ρ_c, and the density contrast is $\zeta = \frac{\rho_f}{\rho_c}$ (Figure 2). Since $l/a \neq 0$ the kink MHD mode is resonantly coupled to Alfvén continuum modes and is damped in time.

For standing kink waves, and without using the thin tube and thin boundary approximation, the normal mode period and damping ratio are functions of the relevant equilibrium parameters,

$$P = P(k_z, \zeta, l/a, v_{Af}), \qquad \frac{P}{\tau_d} = \frac{P}{\tau_d}(k_z, \zeta, l/a),$$

with v_{Af} the thread Alfvén speed. In the thin tube and thin boundary approximations (TTTB), the period does not depend on l/a and the damping ratio is independent of the wavelength. For prominence threads, the wavelength of oscillations needs to be measured and the above relations indicate that, if no assumption is made on any of the physical parameters of interest, there are infinite different equilibrium models that can equally well explain the observations (namely the period and damping ratio). The parameter values that define these valid equilibrium models are displayed in Figure 3, where the analytical algebraic expressions in the TTTB approximations by Goossens *et al.* (2008) have been used to invert the problem. It can be appreciated that, even if an infinite number of solutions is obtained, they define a rather constrained range of values for

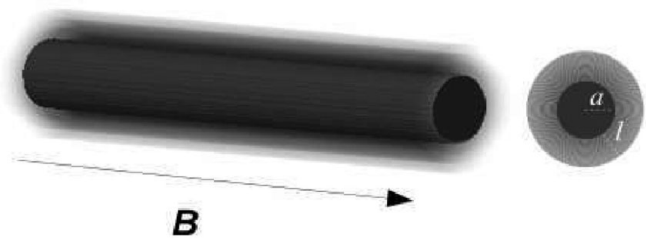

Figure 2. Radially non-uniform filament fine structure [Arregui *et al.* (2008)].

https://doi.org/10.1017/S1743921313010703 Published online by Cambridge University Press

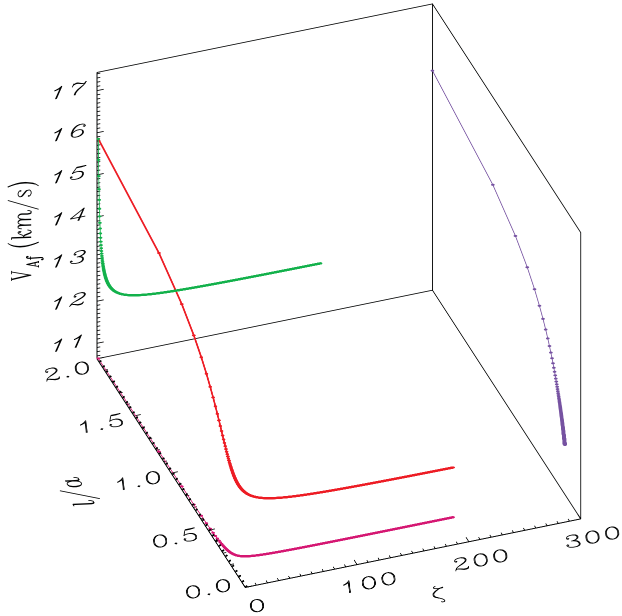

Figure 3. Analytic inversion of physical parameters in the $(\zeta, l/a, v_{Af})$ space for a filament thread with $P = 3$ min., $\tau_d = 9$ min. and a wavelength $\lambda = 3000$ km. [Arregui *et al.* (2012)]

the thread Alfvén speed. Because of the insensitiveness of the damping rate with the density contrast for the typically large values of this parameter in prominence plasmas, the obtained solution curve displays an asymptotic behaviour for large values of ζ. This makes possible to obtain precise estimates for the thread Alfvén speed, $v_{Af} \simeq 12$ km/s and the transverse inhomogeneity length scale, $l/a \simeq 0.16$. The computation of the magnetic field strength from the obtained seismological curve requires the assumption of a particular value for either the filament or the coronal density. In the inversion curve displayed in Figure 3, a change in the period produces a vertical shift of the solution curve, hence the period influences the inferred values for the Alfvén speed.

The main shortcoming of this technique is the use of thread models in which the full magnetic tube is filled with cool and dense plasma. An example of the inversion of physical parameters for different values of the thread length (L_p) was presented by Soler *et al.* (2010). When partially filled threads, i.e., with the dense part occupying a length shorter than the total length of the tube L, are considered, one curve is obtained for each value of the length of the thread. Even if each curve gives an infinite number of solutions, again, each of them defines a rather constrained range of values for the thread Alfvén speed, and the ratio L_p/L is a fundamental parameter in order to perform an accurate seismology of prominence threads, since different curves produce different estimates for the prominence Alfvén speed. Because of the insensitiveness of the damping ratio with respect to the length of the thread, all solution curves for different lengths of the threads produce the same projection onto the $(\zeta,\ l/a)$-plane. Hence, the same precise estimates of the transverse inhomogeneity length scale obtained from infinitely long thread models are valid, irrespective of the length of the thread. The computation of the magnetic field strength from the obtained seismological curve requires the assumption of a particular value for either the filament or the coronal density.

Recently, and using Bayesian inference, a consistent solution for the inversion problem and the correct propagation of errors from observations to inferred parameters has been

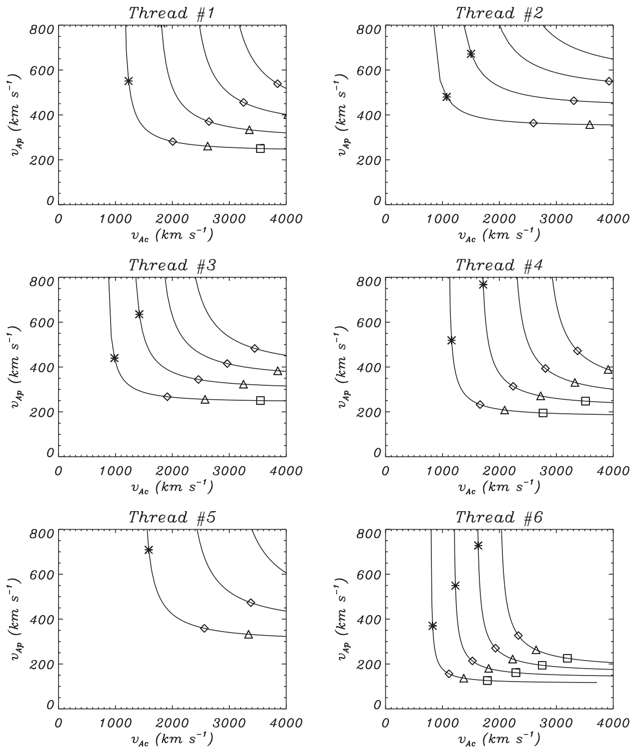

Figure 4. Dependence of the Alfvén velocity in the thread as a function of the coronal Alfvén velocity for the six threads observed by Okamoto *et al.* (2007). In each panel, from bottom to top, the curves correspond to a length of magnetic field lines of 100,000 km, 150,000 km, 200,000 km and 250,000 km, respectively. Asterisks, diamonds, triangles and squares correspond to ratio of the thread to the coronal one $\zeta \simeq 5, 50, 100, 200$. From Terradas *et al.* (2008).

proposed [Arregui *et al.* (2013), Arregui & Asensio Ramos, (2011)]. Using the same values as before and considering an uncertainty in time-scales of the order of 0.1 min. [Lin *et al.* (2009)], they obtained

$$v_{Ap} = 11.9 \pm 0.4\ km/s; \quad l/a = 0.21 \begin{cases} +0.001 \\ -0.002 \end{cases}$$

3.2.3. *Seismology of flowing and oscillating prominence threads*

The first application of prominence seismology using Hinode observations of flowing and transversely oscillating threads was presented by Terradas *et al.* (2008) using observations obtained in an active region filament by Okamoto *et al.* (2007).

The observations show a number of threads that flow following a path parallel to the photosphere while they oscillate in the vertical direction. The relevance of this particular event is that the coexistence of waves and flows can be firmly established, so that there is no ambiguity about the wave or flow character of a given dynamic feature: both seem to be present in this particular event.

In their seismological analysis of these oscillations Terradas *et al.* (2008) started by neglecting the mass flows. Then, they interpreted these events in terms of the standing kink mode of a finite-length thread in a magnetic flux tube. By using theoretical results by Díaz *et al.* (2002) and Dymova & Ruderman *et al.* (2005), Terradas *et al.* (2008) found that a one-to-one relation between the thread Alfvén speed and the coronal Alfvén speed could be established. This relation comes in the form of a number of curves relating the two Alfvén speeds for different values of the length of the magnetic flux tube and the density contrast between the filament and coronal plasma (Figure 4). An interesting property of the obtained solution curves is that they display an asymptotic behaviour for large values of the density contrast, which is typical of filament to coronal plasmas, and hence a lower limit for the thread Alfvén speed can be obtained. Take for instance thread 6. Considering a magnetic flux tube length of 100 Mm, a value of 120 km/s for the thread Alfvén speed is obtained.

Terradas *et al.* (2008) next incorporated mass flows into their analysis by considering the numerical solution of the non-linear, ideal, low-β MHD equations. The numerical results indicate that the effect of the flow on the obtained periods is weak. In fact, using the flow velocities measured by Okamoto *et al.* (2007) slightly shorter kink mode periods than the ones derived in the absence of flow are obtained. Differences are small, however, and produce period shifts between 3 and 5% and, therefore, on the derived Alfvén speed values. We must note that in this case, and because of the small value of the flow speeds measured by Okamoto *et al.* (2007) in this particular event, there are no significant variations of the wave properties, and hence of the inferred Alfvén speeds.

More extensive information about seismological techniques can be found in Arregui *et al.* (2012)

4. Conclusions

Up to now, MHD seismology has not been used to interpret large amplitude oscillations. On the contrary, these oscillations have been explained in terms of oscillators whose restoring forces are magnetic tension, magnetic pressure gradient or projected gravity, and the performed seismology has been based in the analysis of these oscillations. On the other hand, following the analysis by Ruderman & Goossens (2013) about nonlinear kink oscillations in coronal magnetic loops, the ratio between the displacement and the radius (thickness) of a magnetic flux tube (slab) determines whether the transverse oscillations are linear or not. Taking this analysis into account, most of the large amplitude transverse oscillations observed in filaments could be nonlinear, therefore, this should be taken into account when setting up theoretical models to explain these oscillations.

In the case of small amplitude oscillations, prominence seismology is based on evidence of MHD waves and highly idealized theoretical models, in particular with respect to the magnetic configuration. Therefore, it is still a young science. However, and in spite of this, tentative values for unknown physical parameters (Alfvén speed, transverse inhomogeneity length scale) in prominence fine structures can be obtained.

An important step ahead for prominence seismology would be to couple radiative transfer with magnetohydrodynamic waves as a mean to establish a relationship between velocity, density, magnetic field and temperature perturbations, and the observed signatures of oscillations like spectral line shift, width and intensity (See Zapior *et al.* in this volume). Also, partial ionization is another topic of interest since, apart from influencing the behaviour of magnetohydrodynamic waves, it poses an important problem for prominence equilibrium models since cross-field diffusion of neutral atoms can give place to flows and drain prominence material. However, the study of the oscillatory behaviour of a fully three-dimensional and dynamical prominence model involving magnetic equilibrium, radiative transfer, etc., seems to be still a dream.

Acknowledgements JLB acknowledges the support from MINECO and FEDER Funds through grant AYA2011-22846 and from CAIB through the "grups competitius" scheme and FEDER Funds.

References

Arregui, I., Terradas, J., Oliver, R., & Ballester, J. L. 2008, *ApJ*(Letters), **682**, L141

Arregui, I. & Asensio Ramos, A. 2011, *ApJ* (Letters), **740**, 44

Arregui, I., Oliver, R., & Ballester, J. L. 2012, *Living Reviews in Solar Physics*, **9**, 2

Arregui, I., Asensio Ramos, A., & Pascoe, D. J. 2013, *ApJ*, **769**, L34

Díaz, A. J., Oliver, R., & Ballester, J. L. 2002, *ApJ*, **580**, 550

Dymova, M. V. & Ruderman, M. S. 2005, *Solar Phys.*, **229**, 79

Engvold, O. 1998, in D. F. Webb, B. Schmieder, & D. M. Rust (eds.) *New Perspectives in Solar Prominences*, Proc. IAU Colloq. No. 167 (San Francisco, ASP), p. 23

Engvold, O. 2008, in R. Erdélyi, & C. A. Mendoza-Briceño (eds.) *Waves & Oscillations in the Solar Atmosphere*, Proc. IAU Symp. No. 247 (San Francisco, ASP), p. 152

Goossens, M., Arregui, I., Ballester, J. L., & Wang, T. J. 2008, *A & A*, **484**, 851

Hyder, C. L. 1966, *ZfA*, **63**, 78

Isobe, H. & Tripathi, D. 2006, *A & A*, **449**, L17

Jing, J., Lee, J., Spirock, T. J., Xu, Y., Wang H., & Choe, G. S. 2003, *ApJ* (Letters), **584**, L103

Jing, J., Lee, J., & Spirock, T. J., Wang H. 2006, *Solar Phys.*, **236**, 97

Joarder, P. & Roberts, B. 1993, *A & A*, **277**, 225

Kleczek, J. & Kuperus, M. 1969, *Solar Phys.*, **6**, 72

Lin, Y. 2004, *Ph.D. Thesis*, University of Oslo, Norway

Lin, Y., Engvold, O., Rouppe Van der Voort, L. H. M., Wiik, J. E., & Berger, T. E. 2005, *Solar Phys.*, **225**, 229

Lin, Y., Engvold, O., Rouppe Van der Voort, L. H. M., & Van Noort, M. J. 2007, *Solar Phys.*, **246**, 65

Lin, Y., Martin, S. F., Engvold, O., Rouppe Van der Voort, L. H. M., & Van Noort, M. J. 2003, *Adv. Sp. Res.*, **42**, 803

Lin, Y., Soler, R., Engvold, O., Ballester, J. L., Langagen, O., Oliver, R., & Rouppe Van der Voort, L. H. M. 2009, *ApJ*, **704**, 870

Luna, M. & Karpen, J. 2012, *ApJ* (Letters), **750**, L1

Luna, M., Díaz, A. J., & Karpen, J. 2012, *ApJ* (Letters), **757**, L98

Okamoto, T. J., Tsuneta, S., Berger, T. E., Ichimoto, K., Katsukawa, Y., Lites, B. W., Nagata, S., Shibata, K, Shimizu, T., Shine, R. A., Suematsu, Y., Tarbell, T. D., & Title, A. M. 2007, *Science*, **318**, 1577

Pintér, B., Jain, R., Tripathi, D., & Isobe, H. 2008, *ApJ* **680**, 1560

Pouget, G., Bocchialini, K., & Solomon, J. 2006, *A & A* **450**, 1189

Ramsey, H. E. & Smith, S. F. 1966, *AJ*, **71**, 197

Régnier, S.,Solomon, J., & Vial, J. C. 2001, *A & A*, **376**, 292

Roberts, B. & Joarder, P. 1994, in G. Belvedere, M. Rodon, & G. M. Simnett (eds.) *Advances in Solar Physics*, Proc. seventh European Meeting on Solar Physics (Lecture Notes in Physics 432, Springer), p. 173 *ARAA*, **41**, 241

Roberts, B., Edwin, P. M., & Benz, A. O. 1984, *ApJ*, **279**, 857

Rosenberg, H. 1970, *A & A*, **9**, 159

Ruderman, M. & Goossens, M. 2013, *Solar Phys.* (In press)

Soler, R., Arregui, I., Oliver, R., & Ballester, J. L. 2010, *ApJ*, **722**, 1778

Terradas, J., Arregui, I., Oliver, R., & Ballester, J. L. 2008, *ApJ*(Letters), **978**, L153

Tripathi, D., Isobe, H., & Jain, R. 2009, *Space Sci. Revs*, **149**, 283

Uchida, Y. 2004, *PASJ*, **22**, 341

Vial, J. C. 1998, in D. F. Webb, B. Schmieder, & D. M. Rust (eds.) *New Perspectives in Solar Prominences*, Proc. IAU Colloq. No. 167 (San Francisco, ASP), p. 175

Vršnak, B., Veronig, A. M., Thalman, J. K., & Žic, T. 2007, *ApJ*, **647**, 676

Zhang, Q. M., Chen, P. F., Xia, C., Keppens, R., & Ji, H. S. 2013, *A & A*, **554**, A124